Published in final edited form as:
J Control Release. 2010 November 1; 147(3): 400–407. doi:10.1016/j.jconrel.2010.08.019.

Device-based local delivery of siRNA against mammalian target of rapamycin (mTOR) in a murine subcutaneous implant model to inhibit fibrous encapsulation

Hironobu Takahashi[a,†,1], **Yuwei Wang**[a,†], and **David W. Grainger**[a,b,*]

Hironobu Takahashi: htakahashi@abmes.twmu.ac.jp; Yuwei Wang: luckwangyuwei@gmail.com; David W. Grainger: David.Grainger@utah.edu

[a] Department of Pharmaceutics and Pharmaceutical Chemistry, University of Utah, Salt Lake City, UT 84112-5820 USA

[b] Department of Bioengineering, University of Utah, Salt Lake City, UT 84112-5820 USA

Abstract

Fibrous encapsulation of surgically implant devices is associated with elevated proliferation and activation of fibroblasts in tissues surrounding these implants, frequently causing foreign body complications. Here we test the hypothesis that inhibition of the expression of mammalian target of rapamycin (mTOR) in fibroblasts can mitigate the soft tissue implant foreign body response by suppressing fibrotic responses around implants. In this study, mTOR was knocked down using small interfering RNA conjugated with branched cationic polyethylenimine (bPEI) in fibroblastic lineage cells in serum-based cell culture as shown by both gene and protein analysis. This mTOR knockdown led to an inhibition in fibroblast proliferation by 70% and simultaneous down-regulation in the expression of type I collagen in fibroblasts *in vitro*. These siRNA/bPEI complexes were released from poly(ethylene glycol) (PEG)-based hydrogel coatings surrounding model polymer implants in a subcutaneous rodent model *in vivo*. No significant reduction in fibrous capsule thickness and mTOR expression in the foreign body capsules was observed. Observed siRNA inefficacy in this *in vivo* implant model was attributed to siRNA dosing limitations in the gel delivery system, and lack of targeting ability of the siRNA complex specifically to fibroblasts. While *in vitro* data supported mTOR knock-down in fibroblast cultures, *in vivo* siRNA delivery must be further improved to produce clinically relevant effects on fibrotic encapsulation around implants.

Keywords

foreign body reaction; fibrous capsule; mTOR siRNA; local delivery; fibrosis; implant

[*]Correspondence: David W. Grainger, Ph.D, Department of Pharmaceutics and Pharmaceutical Chemistry, University of Utah, Salt Lake City, UT 84112-5820 USA, Phone: +1 801-581-3715, Fax: +1 801-581-3674.
[†]Authors contributed equally to the work
[1]Present address: Institute of Advanced Biomedical Engineering and Science Tokyo, Women's Medical University, 8-1 Kawada-cho, Shinjuku-ku, Tokyo 162-8666, Japan, TEL: +81-3-5367-9945 Ext.6224

Introduction

The foreign body reaction (FBR) at the tissue/material interface commonly contributes to abnormal inflammation, wound healing responses and tissue fibrosis without effective mitigation.(1,2) In general, monocytes/macrophages are activated at implant surfaces and modulate local host fibroblast function, contributing to often-excessive deposition of collagen matrix around implanted materials (fibrotic capsule), a component of the FBR.(1,3) Recent work (4) demonstrated that macrophage fusion observed around implants alone does not necessarily produce implant fibrotic encapsulation. Instead, an alternative hypothesis is that fibro-proliferation is regulated by growth factors secreted by activated macrophages.(3,5,6) Fibrogenesis induced by implants is characterized by macrophage activation and associated elevated proliferation and activation of fibroblasts that up-regulate collagen production. Therefore, control of inflammation around implants by locally released drugs to reduce cell activation and limit collagen encapsulation of implanted biomaterials has been reported.(7–9)

Mammalian target of rapamycin (mTOR) plays a critical role in cell cycle regulation. Rapamycin, a known inhibitor for mTOR (10), can inactivate mTOR specifically. Because mTOR regulates cell proliferation, it has been extensively investigated as a potent target for both anti-cancer (11) and anti-restenotic (12) therapies. Inhibition of mTOR in fibroblasts influences not only proliferation but also collagen production.(13,14) Rapamycin and its analogues are reported to effectively prevent cardiac and pulmonary fibrosis *in vivo*. (15,16) These previous reports describing modulation of mTOR in fibroblasts indicate that mTOR could also be a potent target to prevent implant-induced fibrosis in the context of the FBR.

RNA interference (RNAi) is a powerful tool to knock down specific mRNA expression levels by exploiting a natural intracellular regulatory phenomenon in mammalian species.(17–19) Gene silencing using short interfering RNAs (siRNAs) has many potential therapeutic applications.(20) However, RNAi technology has not yet been used clinically useful largely due to challenges in dosing and effective targeted siRNA delivery systems. Local or topical siRNA therapeutics have been most actively investigated and successful delivery approaches include ocular delivery, respiratory delivery, CNS delivery, skin delivery and vaginal delivery where local delivery accesses cell target populations directly.(21–25) One unexplored and promising delivery route is via combination implantable devices for local drug delivery.(26) We therefore demonstrate device-based local delivery of siRNA, testing the hypothesis that delivery of mTOR siRNA from poly(ethylene glycol) (PEG)-based hydrogel-coated biomaterials can suppress collagen encapsulation elicited from a soft tissue implant FBR.

Materials and methods

Chemicals

Branched polyethylenimine (bPEI) (mol. wt.: 25,000) and dithiothreitol (DTT) were obtained from Sigma-Aldrich (USA). Poly(ethylene glycol) dimethacrylate (PEGDM; mol. wt.: 7500) was synthesized as reported previously.(27) RNase-free water was prepared using diethyl pyrocarbonate (DEPC) (Sigma-Aldrich). All siRNA molecules were purchased from Dharmacon (CO, USA).

Preparation of siRNA/bPEI complexes

To prepare siRNA/bPEI complexes at various anion/cation charge (NP) ratios, 2 μl of 10 μM mTOR siRNA aqueous solution (sense: GCG GAU GGC UCC UGA CUA UUU, antisense: AUA GUC AGG AGC CAU CCG CUU) was mixed with 2μl of bPEI solutions of different concentrations (0.016–0.64μg). The complex mixed solutions were kept at room temperature

for 20 minutes. Then 4μl of each mixture was electrophoresed using ethidium bromide-stained TBE-based 2% agarose gels run at 80V for 20min, followed by visualization with UV light to assess the siRNA-bPEI complex formation.

Cell culture and siRNA transfection in vitro

Murine NIH 3T3 fibroblasts (American Type Culture Collection, ATCC) were plated at 3×10^4 cells/well in a 12-well plate in Dulbecco's modified Eagle's medium (DMEM, GIBCO) supplemented with 10% heat-inactivated fetal bovine serum (FBS, Hyclone®, USA) and 1% penicillin-streptomycin (GIBCO), defined for all cell cultures as "complete media", at 37°C with 5% CO_2 overnight. Cell transfections with siRNA/bPEI complexes at fixed NP ratios in complete media were performed subsequently. siRNA/bPEI complexes for each well are prepared by mixing 7ul of 20 μM siRNA aqueous solution with 4.48μl, 2.24μl, 1.12μl and 0μl (NP 20, 10, 5 and 0) of 1mg/ml bPEI, respectively, in a total volume of 18μl with RNase-free water. After incubation at room temperature for 20 minutes, complete media was added to achieve the final volume of 1ml, yielding a final concentration of siRNA in each well of 140nM. Cell siRNA transfections were always performed in complete media. After 24-hour incubation at 37°C under 5% CO_2, culture media was refreshed with 1ml complete media and the transfected cells were further incubated.

Cell cytotoxicity and proliferation

3T3 murine fibroblasts were seeded at 3×10^3 cells/well in 96-well plates in complete media. After overnight incubation, cells were transfected with mTOR siRNA/bPEI complexes at different NP ratios (1, 2, 5, 10, 20, and 40 prepared as described above) in complete media, maintaining siRNA concentration at 140nM. Cytotoxicity of the siRNA/bPEI complexes was determined at 24 hours after initial transfection using the CellTiter 96 Aqueous One Solution Cell Proliferation Assay (Promega, USA). Media for each well was replaced with 100μl fresh complete media containing 20μl of Cell Titer 96 Aqueous One Solution including three wells without cells for background subtraction. Cells were then incubated at 37°C for 2 hours and optical absorbance at 490nm was then determined using a plate reader (TECAN GENIOS Plus).

To evaluate mTOR siRNA effects on cell proliferation, cells were plated at 3×10^4 cells/well in 6-well plates and transfected with mTOR siRNA/bPEI complexes at an NP ratio of 20 in complete media. Non-targeting siRNA/bPEI complexes with the same NP ratio were used as control. Cultures were refreshed with complete media 24 hours later. After incubation at 37° C for 5 days, relative numbers of cells in each well were determined using the Cell Proliferation Assay (Promega, USA). CellTiter 96 solution-containing media was transferred to 96-well plates for optical reading at 490 nm. In addition, cultured cells were imaged at Day 5 with phase contrast microscopy prior to this assay.

Western immunoblotting

Cells were lysed by using M-PER Mammalian Protein Extraction reagent (Pierce, USA) with 1X Halt™ protease inhibitor cocktail (Pierce). Insoluble material was removed by centrifuging at 15,000 rpm at 4°C for 5 min after 20 minutes on ice. Protein concentrations were measured with the Bio-Rad protein assay system (Bio-Rad, USA). Heat-denatured protein samples (8μg) were separated on 4–12% SDS-polyacrylamide gels (Invitrogen) and blotted on to cellulose membranes (Bio-Rad). After blocking with bovine serum albumin (BSA) in phosphate buffered saline containing 0.5% Tween 20 (PBST) for 1 hour at RT, the filter was incubated overnight with antibody against murine mTOR (2983, Cell Signaling) in 5% BSA/PBST with constant shaking. After three washes with PBST, the membrane was incubated with horseradish peroxidase (HRP)-conjugated anti-rabbit IgG (SA1-200, Affinity BioReagents). Housekeeping controls were detected with an antibody against mouse cyclophilin B (PA1-027, Affinity BioReagents) and HRP-conjugated anti-rabbit IgG. Chemiluminescence was

produced with western blotting luminol reagent (Santa Cruz Biotechnology) and gel images captured using a Molecular Imager Gel Doc XR System (Bio-Rad).

Reverse transcript polymerase chain reaction (RT-PCR)

Total RNA harvests from transfected cells were isolated 48 hours after siRNA transfection using an RNeasy Mini Kit (Qiagen). Up to 0.5 μg of RNA was converted to cDNA with the SuperScript III 1st strand RT kit for PCR (Invitrogen). PCR primers were designed for mTOR (forward: 5′-AGC GTA TTG TTG AGG ACT GGC AGA-3′, reverse: 5′-ATC CTG GAG GTT GTT GCC TCT TGA-3′), cyclophilin B (housekeeping control, forward: 5′-GCA ATG GCA AAG GGT TTC TCC ACT-3′, reverse: 5′-AGC GCT TCC CAG ATG AGA ACT TCA-3′), and collagen type 1 alpha 1 (COL1A1) (forward: 5′-AAG AAT GGC GAT CGT GGT GAG ACT-3′, reverse: 5′-TTG AGT CCG TCT TTG CCA GGA GAA-3′) using Primerquest software from Integrated DNA Technologies (IDT, USA). PCR was performed with iTaq DNA polymerase (Bio-Rad), 1.5mM magnesium chloride, 200 μM each of dNTPs, 500nM of each primer, and 2μl of the cDNA. PCR reaction for mTOR was 95°C for 3 min, followed by 25 cycles with 95°C for 30 s, 63.9°C for 30 s, and finally at 72°C for 1 min. PCR reactions for cyclophilin B and COL1A1 were 95°C for 3 min, followed by 30 cycles with 95°C for 30 s, 60°C for 30 s, and finally at 72°C for 1 min. PCR products were collected for all three genes and electrophoresed using ethidium bromide-stained TBE-based 2% agarose gels run at 100V for 30min.

Preparation of PEG-based hydrogel release matrix and in vitro controlled release of siRNA/bPEI complexes to cultured cells

Crosslinked hydrogels releasing siRNA were prepared using PEGDM and DTT at a 1:1 stoichiometric ratio of thiols to acrylates by Michael-type addition reactions.(28,29) FITC-labeled siRNA (FITC-siRNA, siGLO® Green, Dharmacon) was used for determining siRNA release kinetics from the PEG-based hydrogels. To encapsulate siRNA in the hydrogels, 2μg of siRNA and 4.77μl of 1mg/ml bPEI (NP = 20) were mixed first and incubated at room temperature for 15 minutes. Volumes of stock solutions equal to either 4.25 or 8.5mg of PEGDM and 0.09 or 0.18mg of DTT in RNase-free water were added respectively to the siRNA/bPEI complex mixtures successively in a circular plastic mold with a parafilm bottom (6mm) diameter. Final polymerization volume was adjusted to 20μl with RNase-free water. After 5-hour incubations at 37°C, the resulting hydrogels were used for releasing study after washes with PBS at least three times to remove free siRNA and unreacted reagents.

The siRNA-containing hydrogels were immersed in 1ml of PBS buffer for 14 days, and the supernatant was collected and refreshed at different time points for fluorescence intensity measurements using a plate reader (TECAN GENIOS Plus, excitation 485nm/emission 528nm). The standard curve was prepared by using FITC-labeled siRNA PBS solutions (0, 0.0125, 0.25, 0.5, 1, and 2μg/ml).

To further confirm that siRNA can be released as intact polyplexes, delivery of siRNA/bPEI complexes to cells was evaluated by incubating fibroblast cultures with hydrogel-released siRNA/bPEI complexes. Hydrogels were incubated in 1ml complete media at 37°C. The complex suspension was collected at several time intervals over 15 days. At each sampling time except the last one, supernatant (1ml) was removed and an equivolume of fresh media was replaced for continued collection. Cells were plated at 3×10^4 cells/well in a 12-well plate and then treated with the collected media. Protein harvested 3 days later was followed by Western blotting.

In vivo subcutaneous siRNA-releasing device implantation

All procedures were conducted as approved by the Institutional Animal Care and Use Committee of the University of Utah. C57/BL-6 female mice (12-week-old, 20–25g, Jackson Laboratories) were maintained in a pathogen-free facility at the University of Utah. Circular Millipore filters (mixed cellulose ester, pore size: 0.45μm, diameter: 4 mm) were coated with siRNA-containing PEG-based hydrogel under sterile conditions in a cell culture hood. PEGDM, DTT and siRNA/bPEI were mixed in a circular plastic mold with a parafilm bottom (6 mm) diameter and then one filter was placed into the middle of the viscous solution. After incubation at 37°C for 5 hours, the resulting hydrogel (6mm diameter, 0.7mm thickness) containing the embedded filter was used for implantation. Mice were anesthetized by intraperitoneal injection of ketamine/xylazine mixture (ketamine: 75mg/kg, xylazine: 25mg/kg). Their backs were shaved and cleaned. Dorsal incisions about 1cm long were made perpendicularly to the longitudinal axis at the same level as the diaphragm with sterilized surgical scissors. Subcutaneous pockets on both sides of incision were created by blunt curved forceps and the hydrogel-coated filters were implanted subcutaneously into the dorsal region of mice essentially as described previously.(4,30) Identical filter pieces covered with PEG-hydrogel without siRNA were used as negative controls. Hydrogels with siRNAs targeting TGF-β1 (sense: GCA ACA ACG CCA UCU AUG AdTdT, antisense: UCA UAG AUG GCG UUG UUG CdTdT) were used as positive controls (sequence sourced from Dr. M. Gonzalez-Juarrero, Colorado State University, showing significant TGF-β1 knock-down efficacy in a chronic pulmonary tuberculosis murine model, unpublished data). Cellulosic (filter paper) circular discs coated with polymer hydrogels containing mTOR-specific siRNAs were compared to both controls. For mTOR siRNA delivery, two doses, 2μg and 10μg per implant, were tested, while a single control TGF-β1 siRNA dose (10μg) was used. After implantation, each surgical incision was closed with standard 4-0 silk sutures. Each mouse received two bilateral implants dorsally of different siRNA doses, providing 4 implants per siRNA per dose. All subjects were euthanized after 2 weeks and surrounding tissues with implants were harvested by necropsy and fixed in 10% neutralized formalin for histological analysis as described below.

Histological analyses and immunohistochemistry

Tissue samples were embedded in paraffin and cut into 5-μm sections after 24 hours' fixation in 10% formalin. Three longitudinal ground sections were generated per sample and were stained with Hematoxylin and eosin (H&E) for cell nuclei and Masson's trichrome (MTS) for collagen encapsulation assessments (conducted at ARUP, University of Utah).(8,31) Capsule thickness for each section was estimated microscopically as the average thickness at six different random locations, and was determined per filter implant as the average thickness of 3 sections per filter explant.

Immunohistochemical staining was performed by ARUP Laboratories (Salt Lake City, UT). Briefly, slides were cut at 4μm, then melted at 55°C to 60°C for 30 minutes, deparaffinized, and rehydrated in graded alcohols (100% × 2, 95% × 2, 70% × 1) for 1 minute each. The following steps were performed on the Ventana XT (Ventana Medical Systems, Tucson, AZ) at 37°C. Slides were deparaffinized with EZ Prep solution on the XT, and pretreated with CC1 solution for 30 minutes (TGF beta) or 60 minutes (m-TOR) on the XT. Primary mTOR antibody were applied for 2 hours (m-TOR 1:300), followed by the secondary antibody for 32 minutes (anti-rabbit IgG, Sigma 1:100). Detection was done by staining with Alkaline Phosphatase Red, and the counterstain was hematoxylin (Ventana) for 4 minutes. Slides were then dehydrated through graded alcohols (70% × 1, 95% × 2, 100% × 2) for 30 seconds each, dipped in 4 changes of xylene, and covered with a coverslip. Negative controls included sections treated with hydrogel without siRNA loading. Microscopic analysis of the FBR was performed independently by two investigators who were not aware of the identity of the samples.

Cell imaging

Live adherent cells and histological images were captured using a Nikon Eclipse TE 2000-U microscope with Photometrics Coolsnap ES camera (Roper Scientific).

Statistical Analysis

ANOVA followed by two-tailed student's *t*-test was used to evaluate significant differences among groups. All *in vitro* experiments were repeated three times. Error bars represent standard error of the mean. Results were considered statistically significant if $p < 0.05$.

Results

Optimization of mTOR siRNA/bPEI complexes and their cytotoxicity

To determine the NP threshold for stable siRNA complex formation, different amounts of bPEI were mixed with 0.14nmol mTOR siRNA at NP ratios of 0, 0.5, 1, 2, 5, 10, and 20. Figure 1a shows migration of siRNA/bPEI complexes by gel electrophoresis. With NP ratios of 0, 0.5 and 1, siRNA bands migrate separately on the gel, indicating uncomplexed excess siRNA. When the NP ratio is equal to 2, the density of the siRNA band is substantially weaker. When the NP ratios are = 5, no siRNA migrates freely in the gel, indicating that all siRNA molecules are initially entrapped in bPEI complexes through electrostatic interactions. Therefore, the complex at NP > 5 should be appropriate for siRNA transfection.

Cytotoxicity from the siRNA complexes in serum-cultured fibroblasts *in vitro* was compared among the different NP ratios (NP = 0–40). As shown in Figure 1b, compared with cells without any treatment, cytotoxicity of the siRNA complexes is negligible when NP ratios are at or less than 20 ($p = 0.18$). In addition, there is no significant difference among the groups for NP ratios ≤ 20.

In vitro mTOR knock-down by siRNA/bPEI complexes on fibroblast cultures

3T3 Fibroblasts transfected with siRNA/bPEI complexes of different NP ratios (0, 5, 10, and 20) were assayed for mTOR expression. Total protein was harvested three days after siRNA treatment. Western blot results showed significant reductions of mTOR expression by siRNA when the NP ratio was 20 (Figure 2a). Furthermore, an NP ratio of 20 is sufficient to knock down mTOR expression in fibroblasts *in vitro* using serum-based transfections. Therefore, the effect of mTOR siRNA/bPEI complexes on cellular mTOR gene expression was only evaluated by RT-PCR for NP = 20. Non-targeting siRNA/bPEI complexes with the same NP ratio were used as controls. Compared to controls, mTOR siRNA complexed with bPEI reduces mTOR mRNA expression dramatically (Figure 2b) in 3T3 fibroblast cultures *in vitro*.

Since mTOR positively regulates collagen type I production,(13) COL1A1 mRNA levels were also assayed after mTOR siRNA transfection. Compared with non-targeting siRNA transfection, COL1A1 mRNA levels were significantly suppressed by mTOR siRNA treatment *in vitro* (Figure 2c).

mTOR siRNA effects on cell proliferation in vitro

Cell proliferation assays were performed 5 days after siRNA transfections in serum-based cultures. As shown in Figure 3c, cell numbers in mTOR siRNA groups under NP ratio 20 are much less than that for control siRNA transfection groups (<30%, $*p = 0.028$). Its representative microscopic images of fibroblasts for control (Figure 3a) and treated (Figure 3b) groups also demonstrate significant differences in cell density.

Release of siRNA encapsulated in PEG-based hydrogels

PEG-based hydrogels were made with published methods (29) by reacting aqueous solutions of PEGDM and DTT. Within a 20μl total reaction volume and an NP ratio of siRNA/bPEI equal to 20, 10μg of siRNA is found to be the maximum loading for successful *in situ* gelation with Michael addition network chemistry. Release profiles for siRNA within the PEG-based hydrogels for two different siRNA/PEG gel formulations were analyzed (Figure 4a). In Formulation 1 (PEGDM: 4.25 mg, DTT: 0.09 mg), approximately 50% of the siRNA was released from the gel within the first 24 hours incubation, and 80% of the siRNA was released within 3 days. In Formulation 2 (PEGDM: 8.5 mg, DTT: 0.18 mg), approximately 80% of the siRNA was released by day 7. A prolonged protein knock-down effect (up to one week) was also obtained by siRNA Formulation 2 compared with Formulation 1 (three days), which was also supported by Western blot results (Figure 4b). Formulation 2 provides longer sustained release kinetics and protein expression suppression, and therefore was used for gel preparations for *in vivo* studies in subdermal implant-based siRNA release in mice.

In vivo implantation of siRNA-releasing hydrogel-coated devices

Tissue harvests surrounding hydrogel-coated filter implants were stained with MTC to identify collagen capsules (blue color). Collagen capsule thicknesses were calculated and compared among negative controls (hydrogels without siRNA: 71.95 ± 7.39 μm), positive controls (hydrogels loaded with TGF β1-specific siRNA: 66.82 ± 10.46 μm) and treated groups (hydrogels loaded with mTOR-specific siRNA: 2 μg dose, 96.60 ± 19.80μm; 10μg dose, 63.22 ± 5.95μm). Collagen capsule structure and thickness were evaluated from microscopic images (see Figure 5, foreign body capsules are demarcated with arrows). However, no significant difference in capsule thickness or structure between these three groups was evident. In addition, H&E staining images indicate that mTOR siRNA does not significantly influence fibroblast density around these implants. To further investigate whether mTOR inhibition modulates the fibrotic response, tissue mTOR expression was evaluated by immunohistochemistry. Immunostaining of mTOR in tissues adjacent to the capsule (2μg and 10μg siRNA dosing cohorts) indicated no significant differences in mTOR expression in foreign body capsules between siRNA-treated mice and the mice treated with blank gel. As shown in Figure 6, foreign body capsules contain fibroblasts, inflammatory cells and ECM. After two-week implantations, no significant foreign body giant cells (FBGC) are observed around the implants. Numbers of macrophages were recruited to the interface, but there were no significant differences in numbers of macrophages around the implants among the groups. Therefore, despite *in vitro* knock-down success, it was concluded that mTOR siRNA treatments produced no significant reductions in FBR capsule thickness and protein knock-down *in vivo*.

Discussion

siRNA is of substantial current interest as a sequence-specific post-transcriptional gene silencing tool for the genetic analysis and, significantly, for translational, therapeutic applications in various mammalian cells.(32,33) In order to overcome several delivery challenges for siRNA in therapeutics, several approaches have been used, including conjugating siRNA with cholesterol (34), and delivery using cationic liposomes (35) and polymer carriers.(36) Some have also been successfully utilized for systemic siRNA delivery in mice.(35,37) Viral vectors have been described for siRNA delivery as well.(38–40) Nevertheless, overcoming viral vector oncogenicity and immunogenicity remains a significant barrier for viral-based siRNA delivery. In general, efficiently targeting siRNA to systemic disease sites remains a significant problem. To overcome this, lipid or polymer-based siRNA delivery systems have been successfully used for local siRNA (e.g., topical) delivery, particularly to ophthalmic, vaginal, dermal, liver, neural, pulmonary and tumor targets.(21, 23–25,41–45) Therefore, locally delivered siRNA from the surface of implantable

subcutaneous devices was assessed for efficacy in targeting a major clinical complication of the foreign body response – implant-associated fibrosis.

To facilitate released siRNA internalization by mammalian cells in serum, mTOR siRNA was complexed with bPEI at different NP ratios (0–20) because of its known utility as a non-viral nucleic acid delivery vector.(46–48) The siRNA/bPEI migration assay (Figure 1a) demonstrates that siRNA forms stable complexes with bPEI when the NP ratio ≥ 5. Cytotoxicity from siRNA complexes was analyzed by culturing fibroblasts with siRNA complexes with different NP ratios up to 40 in serum complete media. Significant cytotoxicity was observed only when the NP ratio approached 40. Taken together, these results indicate that siRNA/bPEI complexes can be used for specific suppression of mTOR expression in fibroblast serum-based cultures for NP ratios from 5 to 20.

Transfection of mTOR siRNA in 3T3 fibroblasts in serum-based cultures produced mTOR gene silencing monitored by Western blotting three days post-transfection. Knock-down of mTOR occurs only when the NP ratio was 20, indicating that siRNA specifically knocked down mTOR message RNA in fibroblasts. To further exclude the possibility of non-specific knockdown of mTOR by the transfection reagent (bPEI), target gene expression was compared between non-targeting siRNA and mTOR siRNA in cells. Compared to non-targeting siRNA complexes, mTOR siRNA complexes reduced mTOR mRNA expression in fibroblasts dramatically as shown in Figure 2b. Thus, these data confirm that mTOR siRNA suppressed the targeted gene specifically through the RNAi mechanism.

In previous studies, mTOR was demonstrated to be essential for activating expression of the collagen type I gene (COL1A1) in dermal fibroblasts.(13,30) A dramatic decrease (75%) in COL1A1 mRNA expression was induced by down-regulating mTOR expression level to 56%. (13) Hence, it is not surprising that mTOR siRNA also down-regulates COL1A1 mRNA expression by decreasing mTOR expression (Figure 2c). This supports the hypothesis that collagen production by fibroblasts would be blocked by mTOR siRNA transfection.

A significant role for mTOR is also promoting cell growth and proliferation by regulating protein synthesis. (49,50) It is therefore conceivable that mTOR knockdown may also control or alter cell proliferation to some extent. Suppression of cell proliferation is shown after fibroblast transfection with mTOR siRNA in cultures (Figure 3). Nearly 70% decrease in cell number after mTOR siRNA treatment is observed compared to non-targeting siRNA transfections, supporting that mTOR function specifically, not cytotoxicity, was successfully suppressed by the specific siRNA delivery to fibroblast cultures in serum.

These *in vitro* findings support siRNA targeting of mTOR to modulate collagen production and implant encapsulation, analogous to rapamycin's use against mTOR as an anti-fibrotic agent.(51–54) To move this *in vivo*, a local delivery strategy using release from an implant surface as a combination device model was used. PEG-based hydrogels were exploited for this *in vivo* delivery system since the Michael addition chemistry in water allows mild *in situ* polymerization at physiological temperatures and pH in the presence of siRNA/bPEI complexes, control of both loading and release rates, and *in situ* polymerization on or around an implant.(28,29) To facilitate siRNA entry into cells, bPEI is used as a known complexing agent for nucleic acid delivery.(47,55) SiRNA/bPEI complexes were loaded into and released from the swollen and degrading PEG-based hydrogel networks. Two different siRNA diffusion profiles were obtained from PEG hydrogels of two formulations, showing that encapsulated siRNA dosing release depends on hydrogel cross-linking. The higher cross-linked PEG hydrogels showed sustained release of siRNA to 14 days *in vitro* (Figure 4a). In addition, the sustained siRNA release resulted in prolonged protein knock-down to 7 days. Furthermore,

this successful knock-down confirms that the released siRNA is active and complexed with PEI. Therefore, siRNA formulation 2 was selected for our *in vivo* studies.

Since encapsulated siRNA molecules exhibit both sustained release from PEG-based hydrogels and effective mTOR and collagen knock-down in the presence of serum *in vitro*, the siRNA hydrogels were applied to a model soft tissue implant to reduce collagen expression and fibroblast proliferation in the context of the FBR. Based on *in vitro* release data showing complete siRNA release after two weeks, implants were harvested two weeks post-surgery. The thickness of the collagen fibrous capsule was evaluated for model circular membrane devices coated with PEG hydrogels in mice. As shown in Figure 5, no significant differences in collagen capsule formation were found among the three groups. Compared to negative controls, both mTOR and control TGF-β siRNA-releasing material groups exhibited no detectable anti-fibrotic activity *in vivo*. The capsule thickness for negative control groups is comparable to the published data for the same cellulose implants harvested four weeks post-surgery in the same animal model, (i.e., 63 ± 25μm in Ref.(4), and 79 ± 40μm in Ref (56)). Previous studies have demonstrated that TGF-β is a potent target for anti-fibrotic therapy. (55,57–59) These studies show anti-fibrotic efficacy of TGF-β siRNA to prevent fibrosis *in vivo* using different delivery systems. However, TGF-β siRNA showed no detectable anti-fibrotic activity as collagen capsule thickness was unaffected by the TGF-β siRNA in the murine implant model. Possible explanations for these non-distinguishing results include insufficient siRNA dosing, inefficient cellular uptake by the target fibroblasts around the implant, and siRNA scavenging by cells other than fibroblasts at the implant site. A limitation of this design is that PEG hydrogel gelation is inhibited when siRNA complex loading exceeds 10μg per polymerization. siRNA device-based dose loading cannot be increased in this formulation to address the dosing issue *in vivo*. Effective gene silencing dose of siRNA in many applications in vivo is 1–2.5mg/kg.(21) Here, our study administered 0.4~0.5mg/kg. Thus, inefficient silencing produced by the siRNA was due partially to low dosing. As bPEI also has mild nucleophilicity and some Michael addition capability with PEG acrylate,(60) increasing bPEI concentrations in the gelation step could alter polymerization and also affect bPEI participation as a cell transfection agent.

In situ tissue slice histology immunostaining for mTOR protein was performed to monitor in vivo knock-down effects. In both 10μg and 2μg mTOR siRNA dose-treated groups, siRNA treatment is unable to inhibit mTOR protein expression in the capsule. Therefore, similar capsule thickness results from unchanged mTOR expression level in fibroblasts. For subcutaneous filter paper implantation in our case, FBGCs were difficult to find at the implant interface with tissue two-week post-implantation. Plenty of macrophages were recruited to the interface, however, there is no significant difference of the number of macrophages at the implant and capsule interface between siRNA treated groups and controls. Immunoreactivity appears comparable in all groups and the addition of siRNA does not elicit significant changes in the FBR. In the early stage of the FBR, macrophages recruited to the implant site fuse to form FBGCs. They adhere to the surface of the hydrogel-coated implant and release several chemicals that affect the implant surface. In this microenvironment, the hydrogel was also susceptible to degradation. Some fraction of siRNA/PEI complexes are likely taken up by active capsule-associated cell endo- and phagocytosis mechanisms, followed by their degradation in phagolysosomes where pH remains as low as 4.(61) Hydrogel-released siRNA/PEI complexes escaping active cell phagocytosis must penetrate the dense tissue extracellular matrix in the capsule to approach and enter target cells and then successfully escape endosomes to produce siRNA bioactivity. Hence, despite local siRNA dosing and direct release into the fibrous implant-associated capsule, siRNA polyplex dosing has low percentage success in producing efficacy for mTOR knock-down in vivo. The apparent absence of protein knock-down in vivo is a testimony to the difficulty in getting sufficient siRNA from the implant to nearby fibroblast cells in the capsule. For device-based local siRNA delivery, the drug release

system must overcome non-specific macrophage/FBGC capture and degradation, unless these cells are specific targets for therapies. Therefore, device-based local siRNA delivery seeking to target collagen-producing local fibroblasts, but lacking specific cell-targeting features for fibroblasts, exhibits poor in vivo subcutaneous performance despite promising in vitro knock-down and anti-proliferative efficacy in serum-based fibroblast monocultures.

Conclusions

In vitro cell culture results support siRNA targeting of mTOR to effectively suppress fibroblast proliferation and down-regulate type I collagen mRNA expression in serum-based fibroblast cultures. Thus, like commonly studied rapamycin, mTOR-targeted siRNA was expected to inhibit fibrotic responses around implants *in vivo*. Nonetheless, subcutaneous *in vivo* results demonstrated little translation of *in vitro* siRNA activity to alter implant-associated fibrous encapsulation using a PEG-based hydrogel-coated implant releasing mTOR siRNA in a murine subcutaneous implant model. Though mTOR remains a potent and attractive target for this therapeutic purpose, and local device-based delivery is attractive for combination device local siRNA delivery, further studies are warranted to improve in vivo efficacy in this application. These include new *in vivo* siRNA delivery systems, improvements in siRNA cell transfection efficacy, degradation-resistant siRNA chemistries, and specific siRNA targeting to fibroblasts under physiological conditions and foreign body responses.

Acknowledgments

The authors thank Sheryl Tripp (ARUP, University of Utah) for her immunohistochemical staining expertise, M. Weiser (UCHSC, CO), G. Burns (University of Utah) and, P. Tresco (University of Utah) for technical assistance, and R. J. Christie for providing polymer, PEGDM. This work is partially supported by NIH grant EB000894.

References

1. Ratner BD. Reducing capsular thickness and enhancing angiogenesis around implant drug release systems. J Control Release 2002;78:211–8. [PubMed: 11772462]
2. Anderson JM, Rodriguez A, Chang DT. Foreign body reaction to biomaterials. Semin Immunol 2008;20:86–100. [PubMed: 18162407]
3. Song E, Ouyang N, Horbelt M, Antus B, Wang M, Exton MS. Influence of alternatively and classically activated macrophages on fibrogenic activities of human fibroblasts. Cell Immunol 2000;204:19–28. [PubMed: 11006014]
4. Kyriakides TR, Foster MJ, Keeney GE, et al. The CC chemokine ligand, CCL2/MCP1, participates in macrophage fusion and foreign body giant cell formation. Am J Pathol 2004;165:2157–66. [PubMed: 15579457]
5. Martin P, Leibovich SJ. Inflammatory cells during wound repair: the good, the bad and the ugly. Trends Cell Biol 2005;15:599–607. [PubMed: 16202600]
6. Miller KM, Anderson JM. In vitro stimulation of fibroblast activity by factors generated from human monocytes activated by biomedical polymers. J Biomed Mater Res 1989;23:911–30. [PubMed: 2528547]
7. Norton LW, Koschwanez HE, Wisniewski NA, Klitzman B, Reichert WM. Vascular endothelial growth factor and dexamethasone release from nonfouling sensor coatings affect the foreign body response. J Biomed Mater Res A 2007;81:858–69. [PubMed: 17236219]
8. Blanco E, Weinberg BD, Stowe NT, Anderson JM, Gao J. Local release of dexamethasone from polymer millirods effectively prevents fibrosis after radiofrequency ablation. J Biomed Mater Res A 2006;76:174–82. [PubMed: 16265662]
9. Patil Y, Panyam J. Polymeric nanoparticles for siRNA delivery and gene silencing. Int J Pharm 2009;367:195–203. [PubMed: 18940242]
10. Dumont FJ, Su Q. Mechanism of action of the immunosuppressant rapamycin. Life Sci 1996;58:373–95. [PubMed: 8594303]

11. Law BK. Rapamycin: an anti-cancer immunosuppressant? Crit Rev Oncol Hematol 2005;56:47–60. [PubMed: 16039868]
12. Windecker S, Roffi M, Meier B. Sirolimus eluting stent: a new era in interventional cardiology? Current pharmaceutical design 2003;9:1077–94. [PubMed: 12678859]
13. Shegogue D, Trojanowska M. Mammalian target of rapamycin positively regulates collagen type I production via a phosphatidylinositol 3-kinase-independent pathway. J Biol Chem 2004;279:23166–75. [PubMed: 15047702]
14. Poulalhon N, Farge D, Roos N, et al. Modulation of collagen and MMP-1 gene expression in fibroblasts by the immunosuppressive drug rapamycin. A direct role as an antifibrotic agent? The Journal of biological chemistry 2006;281:33045–52. [PubMed: 16914544]
15. Gao XM, Wong G, Wang B, et al. Inhibition of mTOR reduces chronic pressure-overload cardiac hypertrophy and fibrosis. Journal of hypertension 2006;24:1663–70. [PubMed: 16877971]
16. Simler NR, Howell DC, Marshall RP, et al. The rapamycin analogue SDZ RAD attenuates bleomycin-induced pulmonary fibrosis in rats. Eur Respir J 2002;19:1124–7. [PubMed: 12108867]
17. Hannon GJ, Rossi JJ. Unlocking the potential of the human genome with RNA interference. Nature 2004;431:371–8. [PubMed: 15372045]
18. Jones SW, Souza PM, Lindsay MA. siRNA for gene silencing: a route to drug target discovery. Current opinion in pharmacology 2004;4:522–7. [PubMed: 15351359]
19. Aigner A. Delivery systems for the direct aplication of siRNAs to induce RNA interference (RNAi) in vivo. journal of biomedicine and biotechnology 2006;2006:1–15.
20. de Fougerolles A, Vornlocher HP, Maraganore J, Lieberman J. Interfering with disease: a progress report on siRNA-based therapeutics. Nat Rev Drug Discov 2007;6:443–53. [PubMed: 17541417]
21. Woodrow KA, Cu Y, Booth CJ, Saucier-Sawyer JK, Wood MJ, Saltzman WM. Intravaginal gene silencing using biodegradable polymer nanoparticles densely loaded with small-interfering RNA. Nat Mater 2009;8:526–33. [PubMed: 19404239]
22. Reich SJ, Fosnot J, Kuroki A, et al. Small interfering RNA (siRNA) targeting VEGF effectively inhibits ocular neovascularization in a mouse model. Mol Vis 2003;9:210–6. [PubMed: 12789138]
23. Takanashi M, Oikawa K, Sudo K, et al. Therapeutic silencing of an endogenous gene by siRNA cream in an arthritis model mouse. Gene Ther 2009;16:982–9. [PubMed: 19474812]
24. Massaro D, Massaro GD, Clerch LB. Noninvasive delivery of small inhibitory RNA and other reagents to pulmonary alveoli in mice. Am J Physiol Lung Cell Mol Physiol 2004;287:L1066–70. [PubMed: 15234906]
25. Thakker DR, Natt F, Husken D, et al. Neurochemical and behavioral consequences of widespread gene knockdown in the adult mouse brain by using nonviral RNA interference. Proc Natl Acad Sci U S A 2004;101:17270–5. [PubMed: 15569935]
26. Wu P, Grainger DW. Drug/device combinations for local drug therapies and infection prophylaxis. Biomaterials 2006;27:2450–67. [PubMed: 16337266]
27. Christie RJ, Findley DJ, Dunfee M, Hansen RD, Olsen SC, Grainger DW. Photopolymerized hydrogel carriers for live vaccine ballistic delivery. Vaccine 2006;24:1462–9. [PubMed: 16246467]
28. van de Wetering P, Metters AT, Schoenmakers RG, Hubbell JA. Poly(ethylene glycol) hydrogels formed by conjugate addition with controllable swelling, degradation, and release of pharmaceutically active proteins. J Control Release 2005;102:619–27. [PubMed: 15681084]
29. Metters A, Hubbell J. Network formation and degradation behavior of hydrogels formed by Michael-type addition reactions. Biomacromolecules 2005;6:290–301. [PubMed: 15638532]
30. Kyriakides TR, Zhu YH, Yang Z, Huynh G, Bornstein P. Altered extracellular matrix remodeling and angiogenesis in sponge granulomas of thrombospondin 2-null mice. Am J Pathol 2001;159:1255–62. [PubMed: 11583953]
31. Bryers JD, Jarvis RA, Lebo J, Prudencio A, Kyriakides TR, Uhrich K. Biodegradation of poly (anhydride-esters) into non-steroidal anti-inflammatory drugs and their effect on Pseudomonas aeruginosa biofilms in vitro and on the foreign-body response in vivo. Biomaterials 2006;27:5039–48. [PubMed: 16777217]
32. Aagaard L, Rossi JJ. RNAi therapeutics: principles, prospects and challenges. Adv Drug Deliv Rev 2007;59:75–86. [PubMed: 17449137]

33. Almeida R, Allshire RC. RNA silencing and genome regulation. Trends Cell Biol 2005;15:251–8. [PubMed: 15866029]
34. Soutschek J, Akinc A, Bramlage B, et al. Therapeutic silencing of an endogenous gene by systemic administration of modified siRNAs. Nature 2004;432:173–8. [PubMed: 15538359]
35. Sorensen DR, Leirdal M, Sioud M. Gene silencing by systemic delivery of synthetic siRNAs in adult mice. J Mol Biol 2003;327:761–6. [PubMed: 12654261]
36. Khan A, Benboubetra M, Sayyed PZ, et al. Sustained polymeric delivery of gene silencing antisense ODNs, siRNA, DNAzymes and ribozymes: in vitro and in vivo studies. J Drug Target 2004;12:393–404. [PubMed: 15545089]
37. Sioud M, Sorensen DR. Cationic liposome-mediated delivery of siRNAs in adult mice. Biochem Biophys Res Commun 2003;312:1220–5. [PubMed: 14652004]
38. Rubinson DA, Dillon CP, Kwiatkowski AV, et al. A lentivirus-based system to functionally silence genes in primary mammalian cells, stem cells and transgenic mice by RNA interference. Nat Genet 2003;33:401–6. [PubMed: 12590264]
39. Tomar RS, Matta H, Chaudhary PM. Use of adeno-associated viral vector for delivery of small interfering RNA. Oncogene 2003;22:5712–5. [PubMed: 12944921]
40. Matta H, Hozayev B, Tomar R, Chugh P, Chaudhary PM. Use of lentiviral vectors for delivery of small interfering RNA. Cancer Biol Ther 2003;2:206–10. [PubMed: 12750565]
41. Reich SJ, et al. Small interfering RNA (siRNA) targeting VEGF effectively inhibits ocular neovascularization in a mouse model. Mol Vision 2004;9:210–216.
42. Nakamura H, et al. RNA interference targeting transforming growth factor-β type II receptor suppresses ocular inflammation and fibrosis. Mol Vis 2004;10:703–711. [PubMed: 15475878]
43. Luo MC, Zhang DQ, Ma SW, et al. An efficient intrathecal delivery of small interfering RNA to the spinal cord and peripheral neurons. Mol Pain 2005;1:29. [PubMed: 16191203]
44. Morrissey DV, Lockridge JA, Shaw L, et al. Potent and persistent in vivo anti-HBV activity of chemically modified siRNAs. Nat Biotechnol 2005;23:1002–7. [PubMed: 16041363]
45. Schiffelers RM, Ansari A, Xu J, et al. Cancer siRNA therapy by tumor selective delivery with ligand-targeted sterically stabilized nanoparticle. Nucleic Acids Res 2004;32:e149. [PubMed: 15520458]
46. Park TG, Jeong JH, Kim SW. Current status of polymeric gene delivery systems. Adv Drug Deliv Rev 2006;58:467–86. [PubMed: 16781003]
47. Wang DA, Narang AS, Kotb M, et al. Novel branched poly(ethylenimine)-cholesterol water-soluble lipopolymers for gene delivery. Biomacromolecules 2002;3:1197–207. [PubMed: 12425656]
48. Jiang G, Park K, Kim J, et al. Hyaluronic acid-polyethyleneimine conjugate for target specific intracellular delivery of siRNA. Biopolymers 2008;89:635–42. [PubMed: 18322932]
49. Achenbach TV, Brunner B, Heermeier K. Oligonucleotide-based knockdown technologies: antisense versus RNA interference. Chembiochem 2003;4:928–35. [PubMed: 14523910]
50. Burnett PE, Barrow RK, Cohen NA, Snyder SH, Sabatini DM. RAFT1 phosphorylation of the translational regulators p70 S6 kinase and 4E-BP1. Proc Natl Acad Sci U S A 1998;95:1432–7. [PubMed: 9465032]
51. Wu MJ, Wen MC, Chiu YT, Chiou YY, Shu KH, Tang MJ. Rapamycin attenuates unilateral ureteral obstruction-induced renal fibrosis. Kidney Int 2006;69:2029–36. [PubMed: 16732193]
52. Neef M, Ledermann M, Saegesser H, Schneider V, Reichen J. Low-dose oral rapamycin treatment reduces fibrogenesis, improves liver function, and prolongs survival in rats with established liver cirrhosis. J Hepatol 2006;45:786–96. [PubMed: 17050028]
53. Salminen US, Maasilta PK, Taskinen EI, Alho HS, Ikonen TS, Harjula AL. Prevention of small airway obliteration in a swine heterotopic lung allograft model. J Heart Lung Transplant 2000;19:193–206. [PubMed: 10703697]
54. Poston RS, Billingham M, Hoyt EG, et al. Rapamycin reverses chronic graft vascular disease in a novel cardiac allograft model. Circulation 1999;100:67–74. [PubMed: 10393683]
55. Kim KH, Kim HC, Hwang MY, et al. The antifibrotic effect of TGF-beta1 siRNAs in murine model of liver cirrhosis. Biochem Biophys Res Commun 2006;343:1072–8. [PubMed: 16579972]

56. Puolakkainen P, Bradshaw AD, Kyriakides TR, et al. Compromised production of extracellular matrix in mice lacking secreted protein, acidic and rich in cysteine (SPARC) leads to a reduced foreign body reaction to implanted biomaterials. Am J Pathol 2003;162:627–35. [PubMed: 12547720]

57. Qi Z, Atsuchi N, Ooshima A, Takeshita A, Ueno H. Blockade of type beta transforming growth factor signaling prevents liver fibrosis and dysfunction in the rat. Proc Natl Acad Sci U S A 1999;96:2345–9. [PubMed: 10051644]

58. Kushibiki T, Nagata-Nakajima N, Sugai M, Shimizu A, Tabata Y. Enhanced anti-fibrotic activity of plasmid DNA expressing small interference RNA for TGF-beta type II receptor for a mouse model of obstructive nephropathy by cationized gelatin prepared from different amine compounds. J Control Release 2006;110:610–7. [PubMed: 16378654]

59. Ruiz-de-Erenchun R, Dotor de las Herrerias J, Hontanilla B. Use of the transforming growth factor-beta1 inhibitor peptide in periprosthetic capsular fibrosis: experimental model with tetraglycerol dipalmitate. Plast Reconstr Surg 2005;116:1370–8. [PubMed: 16217481]

60. Kunath K, von Harpe A, Petersen H, et al. The structure of PEG-modified poly(ethylene imines) influences biodistribution and pharmacokinetics of their complexes with NF-kappaB decoy in mice. Pharm Res 2002;19:810–7. [PubMed: 12134951]

61. Haas A. The phagosome: compartment with a license to kill. Traffic 2007;8:311–30. [PubMed: 17274798]

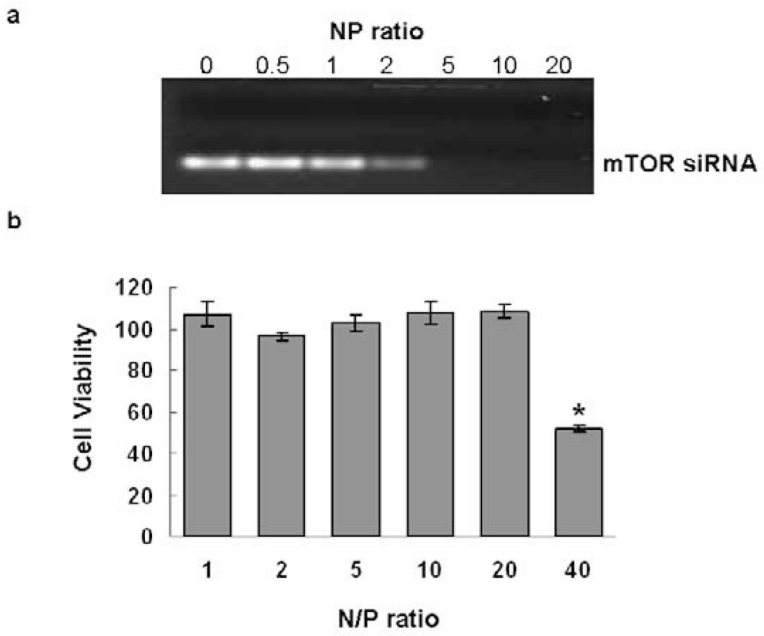

Figure 1.

Gel migration and cytotoxicity assays of mTOR siRNA/bPEI complexes. (a) Gel migration of mTOR siRNA/bPEI complexes at different NP ratios (1–40). (b) Cell cytotoxicity of mTOR siRNA/bPEI complexes in 3T3 fibroblast in serum-based media. Assay was performed 24 hours-post transfection. (*p=0.0004, compared with cultures without treatment).

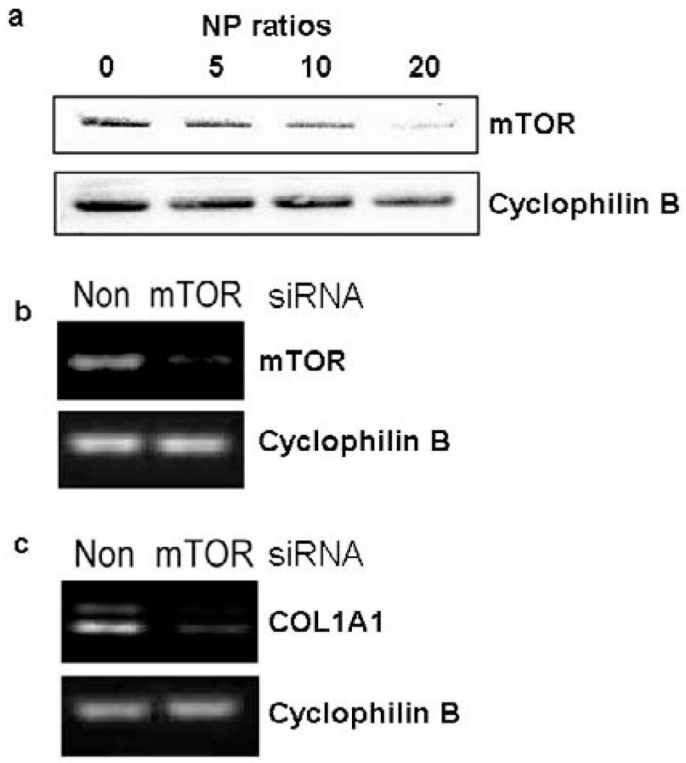

Figure 2.
RNA message knock-down in 3T3 fibroblast cultures in serum-based media. (a) Western blot analysis for mTOR expression after mTOR siRNA/bPEI exposure. Cellular mRNA levels of (b) mTOR and (c) COL1A1 in cells treated with non-targeting siRNA (control) and mTOR siRNA/bPEI complexes were analyzed by RT-PCR. Cyclophilin B (housekeeping gene) mRNA was used as a control.

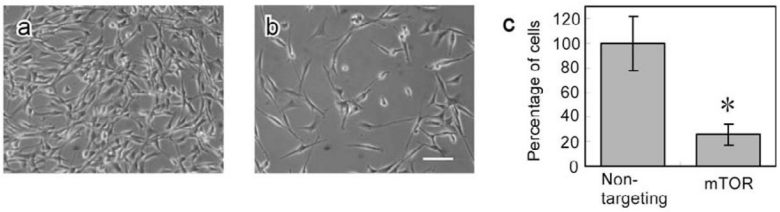

Figure 3.

Microscopic images of fibroblast serum-based cultures (a) treated with non-targeting siRNA, (b) mTOR siRNA at NP ratio 20, and (c) cell proliferation in the siRNA-treated cells (NP 20, *$p = 0.028$), scale bar = 250μm. Images were taken 5 days after siRNA transfection. Numbers of cells treated with non-targeting siRNA was normalized to 100%.

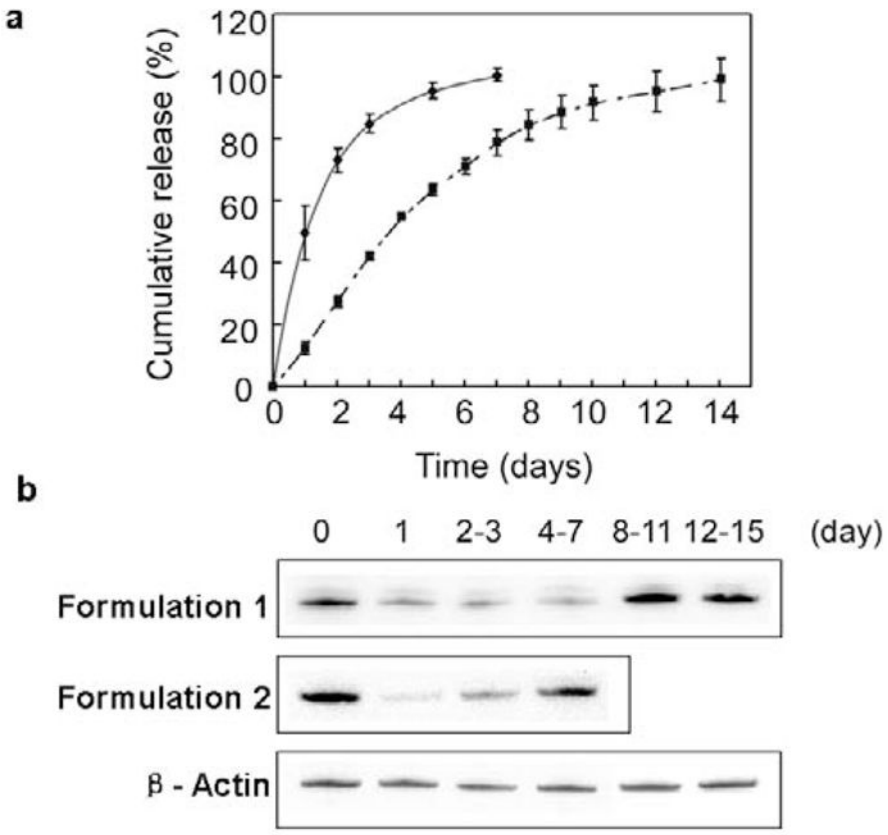

Figure 4.

Release of siRNA/bPEI complex from PEG-based hydrogels *in vitro*. (a) Cumulative siRNA release profiles in PBS media sink conditions. NP ratio of the siRNA/bPEI complex was 20. Release profiles in Formulation 1 (PEGDM: 4.25mg, DTT: 0.09mg) and Formulation 2 (PEGDM: 8.5mg, DTT: 0.18mg) are indicated by the solid line and dash-dotted line, respectively. (b) Western blot analysis for mTOR expression in fibroblasts after incubating cells with hydrogel-released siRNA/bPEI complexes. Cell lysis was harvested after three-day culture in this media. Numbers of days shown reflect the hydrogel release time prior to media collection and cell culture.

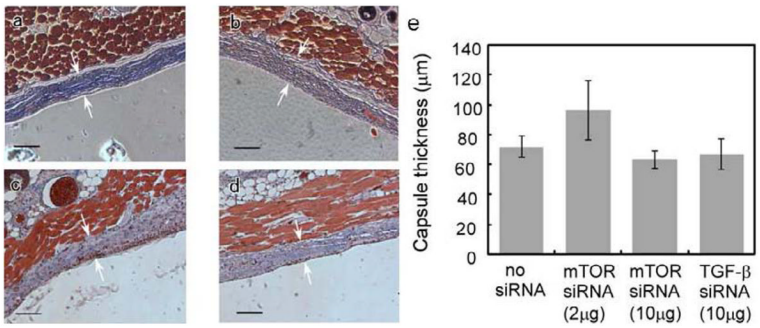

Figure 5.

Comparison of *in vivo* collagen capsule thickness for murine sub-dermal hydrogel-coated implants explanted after two weeks for (a) negative control, no siRNA loaded, (b) 2μg mTOR siRNA loaded, (c) 10μg mTOR siRNA loaded and (d) positive control, 10 μg TGF-β siRNA loaded. Localization of fibrous capsule is marked by white arrows (scale bar = 100μm). (e) Summary of collagen capsule thickness data. P values for each individual group vs. negative control without siRNA treatment are: 0.3112 (2μg mTOR siRNA), 0.3954 (10μg mTOR siRNA), and 0.7045 (10μg TGF-β siRNA).

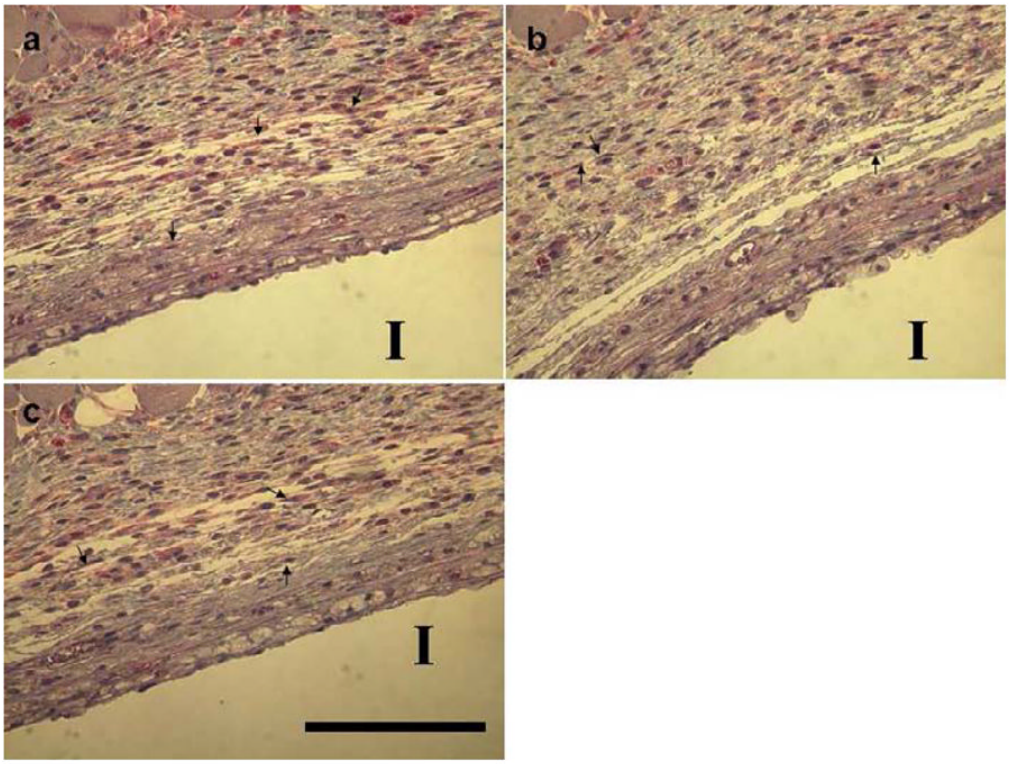

Figure 6.

Immunostains of mTOR protein expression in foreign body capsules from murine histological sections. Tissue samples surrounding implants (I) were harvested from mice two-week post-implantation. Immunohistochemical staining for mTOR in foreign body capsules around filter paper from (a) negative control group (no siRNA loaded), (b) 2μg mTOR siRNA-treated group, and (c) 10μg mTOR siRNA-treated group. Sections were stained with mTOR antibody, and counterstaining was done with hematoxylin. These treatments stain target proteins red and cell nuclei dark (blue). Arrows denote fibroblasts (scale bar = 125μm).